Fracture mechanics of snow avalanches

J. A. Åström and J. Timonen
Department of Physics, University of Jyväskylä, P.O. Box 35, FIN-40351 Jyväskylä, Finland
(Received 22 February 2001; published 22 June 2001)

Dense snow avalanches are analyzed by modeling the snow slab as an elastic and brittle plate, attached by static friction to the underlying ground. The grade of heterogeneity in the local fracture (slip) thresholds, and the ratio of the average substrate slip threshold to the average slab fracture threshold, are the decisive parameters for avalanche dynamics. For a strong pack of snow there appears a stable precursor of local slips when the frictional contacts are weakened (equivalent to rising temperature), which eventually trigger a catastrophic crack growth that suddenly releases the entire slab. In the opposite limit of very high slip thresholds, the slab simply melts when the temperature is increased. In the intermediate regime, and for a homogeneous slab, the model display features typical of real snow avalanches. The model also suggests an explanation to why avalanches are impossible to forecast reliably based on precursor observations. This explanation may as well be applicable to other catastrophic rupture phenomena such as earthquakes.

DOI: 10.1103/PhysRevE.64.011305 PACS number(s): 45.70.Ht, 62.20.Mk, 91.45.Vz, 92.40.Rm

A dense snow or a slab avalanche is distinguished from a loose snow avalanche by the shape of the area that has slid, especially that of the upper edge. A loose snow avalanche typically starts at a single point from which it spreads as pieces of snow tumble down forming a wedge shaped slide surface. The texture of the falling snow is similar to that of soft granular matter. In the slab avalanche, on the other hand, it is rather a large solid plate of dense snow that starts sliding as an intact piece, and then fragments into discrete blocks as it slides down a slope. The boundaries of the snow slab first appear visible as a fracture line on the snow surface at the top of the slab. This fracture line (the so-called crown surface) is typically a shallow wedge opening downwards with its knee at the point in which the failure is initiated. The crown surface usually propagates as far as possible, until eventually a stronger snow pack is encountered and the propagation stops. From this point onwards the fracture line typically continues downhill as a slanting zig-zag pattern, thus forming the flanks of the slab avalanche. Slab avalanches appear almost exclusively on slopes with an inclination in the range $30°-50°$. On steeper slopes thick slabs cannot be formed. Instead, the snow continuously slides downhill as it falls. On more moderate slopes the snow seems only to melt away without any catastrophic events [1,2].

There are entire institutions that monitor the avalanche hazard in countries with a high frequency of avalanches. These institutions usually have advanced semiempirical computer codes to calculate the avalanche risk depending on, e.g., the amount of snow fall, temperature, and wind. There also exist similar computer codes for the flow pattern and run-out distances of avalanches using the mountain-side topology as an input as well as microscopic models of snow packs to investigate their strength [3].

In this article we take another point of view to these phenomena. We consider a snow slab as an elastic plate that is liable to fracture, and anchored to a substrate through static friction. We furthermore assume that there exist uncorrelated fluctuations in both the local slip threshold and the local fracture threshold of the snow slab. We use a random number generator to create virtual snow slabs, and analyze avalanches as a statistical physics system in a fashion typical of fracture mechanics. We focus in particular on their behavior when the grade of heterogeneity is varied together with the ratio of the average slip threshold to the average fracture threshold.

As mentioned above, we consider the snow slab as an elastic and brittle solid. This approximation has been verified experimentally for snow that is deformed at a reasonable strain rate [4,5] (for low strain rates a viscoelastic behavior with ductile creep fracture is a more relevant model). To implement a numerical algorithm we further need to make the solid discrete. We do this by transforming it into a cubic lattice of beams. The intuitive picture is that a beam models the local elastic stiffness in the slab. The discretization is in principle similar to that used in the basic finite-element method. This approach has been tested in Ref. [6]. The beams can be deformed in three dimensions by bending, shearing, stretching, and torsion according to the linear theory of elasticity for slender homogeneous beams. They connect massive blocks (reduced to points) and break if the strain on them exceeds a threshold value. This threshold value is to a large extent determined by the temperature. Cold snow is strong, and its strength vanishes at the melting temperature. This is why most avalanches appear when the temperature is increased close to $0°C$. We take the temperature and thus also the average fracture threshold to be an adjustable parameter.

The slab itself is modeled as a two-dimensional square lattice of beams (its thickness is not relevant here). All sites are connected to the substrate by other beams, the beams thus forming the bonds of a cubic lattice. The connecting ''friction beams'' model the static frictional contact between the substrate and the slab. A gravitational force ($g\rho \sin\theta$) is applied on all the masses in the downhill direction. We assume that the snow slab has a lens shape [7] and adjust the gravitational force accordingly. The slab is anchored at the top and along the sides, thus limiting the size of the avalanche. The dynamical motion of all the lattice sites within the slab are calculated using a discrete version of Newton's equations of motion including a linear damping term,

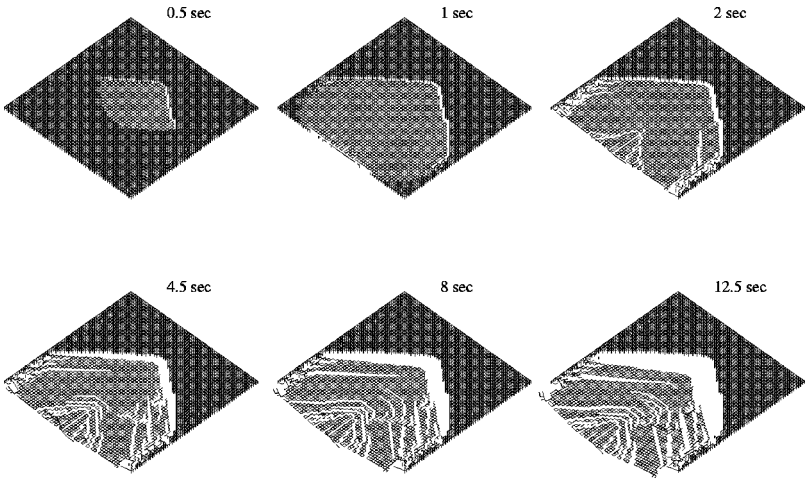

FIG. 1. Snapshots of an avalanche. The time elapsed from the first fracture is indicated at each snapshot.

$$M\ddot{\vec{U}}+C\dot{\vec{U}}+K\vec{U}=\vec{F}. \tag{1}$$

Here $\vec{U}$ is the displacement vector of the lattice sites, K the stiffness matrix, M the mass matrix, C a damping matrix, and $\vec{F}$ the external forces. The time can as well be discretized by using the definition of the time derivative of $\vec{U}$. The time-dependent displacements of the slab sites (i.e., $\vec{U}$) can thereafter be calculated numerically by iteration of time steps, starting from the static equilibrium.

There exist heterogeneities in all natural materials. Both experimental and theoretical investigations have demonstrated that the distribution of strength, e.g., is typically limited to a narrow range [8]. Distributions such as the Weibull $\{C(\tau_c)=1-\exp[c(\tau_c/\tau_s)^m]\}$ or the modified Gumbel $\{C(\tau_c)=1-\exp[-c\exp(-k/\tau_c)]\}$ distribution, which are commonly used to fit experimental data, both display a rapidly decreasing occurrence probability. Schematically, the distribution of local strengths may thus be modeled as a limited uniform distribution of local strengths around an average value. For simplicity, this is what we use here in our numerical model. We denote the distribution of fracture (slip) thresholds by $d(\tau_f)$, and it is thus a nonzero constant in the interval $[1-\delta,1+\delta]$.

In Fig. 1 we show snapshots of a simulation. The slab is homogeneous and a local fracture takes place at a strain that is 1.6 times that needed for a local slip. Initially one single friction beam is removed from the middle of the upper part of the slab, and then the slab is equilibrated. This removed beam models a single perturbation in the substrate. Thereafter the temperature is slowly increased such that the fracture and slip thresholds are simultaneously lowered at a constant rate. The distribution $d(\tau_f)$ thus becomes time dependent. When the fracture and the slip thresholds become sufficiently low, a catastrophic crack propagation within the slab, and simultaneously between the slab and the substrate, takes place. The crack propagation is initiated at the perturbed site. As is evident from Fig. 1, the resulting avalanche is very similar to the real slab avalanches described above.

In order to study in more detail the behavior of the avalanches, we recorded, as functions of time, the total kinetic energy (W_k) and the number of broken beams (N_b) within the slab. To better understand the behavior of N_b, we compare it with an estimate for the number of broken beams based on uncorrelated fracture and on the load distribution before any beams are broken. If the distribution of the initial load on the beams is $p(\tau)$, and the fracture (slip) thresholds decrease linearly with increasing time, as (a_0-at), i.e., when the temperature is increased, then the number of broken beams in the slab can be estimated to be

$$C_b(t)=L_xL_y\int_0^\infty \hat{d}(\tau,t)p(\tau)d\tau, \tag{2}$$

where $\hat{d}(\tau)$ is defined as $\hat{d}(\tau,t)=\int_0^\tau d(\tau_f,t)d\tau_f$.

Our virtual slabs can be categorized into four qualitatively different behaviors depending on the grade of heterogeneity in the local thresholds, and the ratio of the average slip threshold to the average fracture threshold. The characteristics of these four categories are displayed in Fig. 2. In this figure we show N_b, W_k, and C_b as functions of time for the cases when the fracture threshold is large [Fig. 2(A)], the slip threshold is large [Fig. 2(B)], the fracture and the slip thresh-

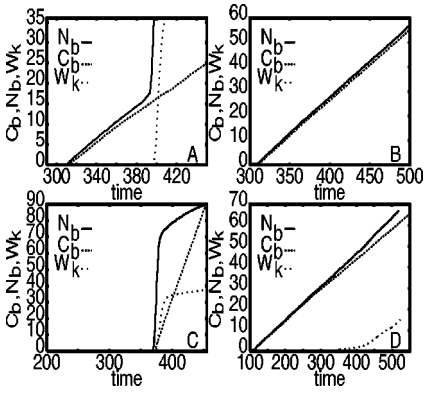

FIG. 2. N_b, C_b, and W_k as functions of time. (A) The strong slab case with $\delta=0.25$, (B) the strong friction case with $\delta=0.25$, (C) the intermediate case with $\delta=0.1$, and (D) the intermediate case with $\delta=0.75$. Notice that W_k coincide with the x axis in (B). The number of broken bonds is given in hundreds on each y axis.

olds are about the same magnitude and the heterogeneity is small [Fig. 2(C)], and correspondingly when the heterogeneity is large [Fig. 2(D)].

In Fig. 2(A) only the friction beams are allowed to break, and $\delta=0.25$. As is evident from Fig. 2(A) the number of broken bonds follows first quite closely the theoretical prediction Eq. (2), while the kinetic energy is practically zero. This number provides a quasistatic precursor to the avalanche. At the time $t\approx 390$, the process becomes unstable and a rapid crack propagating among the friction beams suddenly releases the slab. This phenomenon is reflected in an explosive growth of the kinetic energy, which is increased by more than 7 orders of magnitude in a very short time. For a larger δ the behavior is similar, but the precursor stage is longer. Notice that our model is in this case rather similar to the so-called fiber bundle models [9–11]. The difference is that here there is no need to postulate a load-shearing rule.

In Fig. 2(B), only the slab beams are allowed to break, and $\delta=0.25$. When friction is very strong, and only the slab beams break, the behavior is very different. This would correspond to a layer of snow on a moderate slope. In such a case the normal force on the slab is always much larger than the gravitational force, which means that frictional slips do not appear. No avalanche takes place in this case, the number of broken beams (N_b) practically follows C_b at all times, and the kinetic energy remains very small. The slab simply melts when the temperature is increased.

In Fig. 2(C), the friction beams break at a strain that is 1.6 times that needed for a local slip, and $\delta=0.1$. In this case an avalanche like the one shown in Fig. 1 appears. As demonstrated by this figure, N_b deviates from C_b already when the first beams break at $t\approx 370$. N_b and W_k both increase very rapidly as a result of a catastrophic crack growth that releases the slab. It is only the beams that remain unbroken above the avalanche that break more slowly. This is seen as the more moderate slope of the N_b curve at the end of the simulation.

In Fig. 2(D), the friction beams break at a strain that is 1.6 times that needed for a local slip, and $\delta=0.75$. For delta large, disorder dominates and the number of broken beams follows rather closely the result Eq. (2). The kinetic energy begins to grow gradually as N_b increasingly deviates from C_b. This happens because small fragments of the slab are continuously released from the substrate and they cause local avalanches. This case is similar to creeping failure in the sense that there is no distinct point of global failure.

Precursors have attracted a lot of scientific interest recently as they may provide warning signals for catastrophic events. Observations of precursors in natural snow avalanches have not, however, been conclusive. By submerging microphones in the snow on hazard slopes it has been found that some avalanches give a clear precursor signal in the form of increasing acoustic emission before a large avalanche. On the other hand, many avalanches appear without such signals [12,13]. In the cases in which precursors could be detected, the acoustic emission was found to roughly follow a power-law divergence [12]. We would expect that the kinetic energy of the slab is proportional to the energy of acoustic waves created in the process. Of the four categories in Fig. 2 it is only the one in Fig. 2(A) that displays both a precursor and a catastrophic event. By plotting Fig. 2(A) on a semilogarithmic scale we get a better view of the kinetic energy during this particular event. Figure 3 demonstrates that the kinetic energy is roughly constant before the avalanche. As a comparison we can also make a rough estimate of the kinetic energy based on arguments similar to the ones used to find Eq. (2). This is done by first estimating the elastic energy released in each breaking, and assuming then that this energy is completely transformed into kinetic energy which is dissipated during a constant time interval. This kinetic energy is denoted by E_k in Fig. 3. There is a weak increase in W_k in comparison with E_k just before the avalanche. This increase takes place during a time interval that is about the same as the duration of the avalanche. During this interval the kinetic energy is roughly tripled. This accelerating release of kinetic energy provides the final warning signal for the avalanche. In this particular case the final warning is given at a very short notice, and its energy content is very small in comparison with the enormous amount of energy released in the event itself. Because the kinetic energy increases such that it practically diverges, it is, of course, possible to fit by a power-law curve. We find that $W_k\propto(t_c-t)^{-\alpha}$, with $\alpha=2.5\pm0.5$, just before the onset of the avalanche at $t=t_c$.

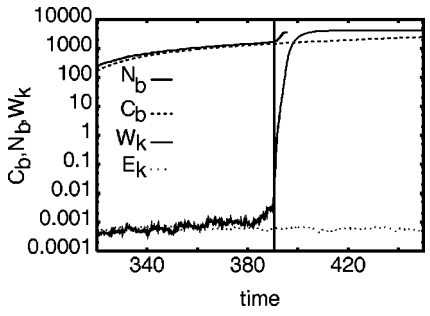

FIG. 3. Figure 2(A) on a semilog scale. E_k is also included for comparison. The vertical line denotes the onset of the avalanche.

How can these results then explain the uncertainty in the occurrence of precursor signals? On one hand, Fig. 2(A) and Fig. 3 display a quasistatic precursor related to microfractures at the weak bonds. The number of friction bonds diminishing because of these micro-fractures, cannot in the end withstand the load of the entire slab, and the avalanche is triggered via an accelerating release of energy. On the other, in Fig. 1 and in Fig. 2(C) there appears initially a dominating load ''hot spot'' at a single site. The first microfracture appeared in the vicinity of this spot and it immediately triggered a catastrophic failure. The avalanches in Figs. 1 and 2(C) thus appeared without any warning signal. It thus seems that the appearance of a precursor signal depends on weather a microfracture is capable of triggering the catastrophic failure, and this depends on a complicated interplay between the distribution of the failure thresholds and the stress field [14]. This interplay has to be determined separately for each weather condition and each slope topology, which makes it very difficult to reliably forecast avalanches based on precursor observations. Finally, there seems to be a similar situation concerning the existence of precursors to earthquakes [15]. Apparently the difficulty there is of similar nature.

[1] D. Sauer, available on the Internet at http://www.firstrax.com/127.htm.
[2] R.I. Perla, Ph.D. thesis, University of Utah, 1971.
[3] P. Bartelt and O. Buser, Phys. World **14**, (2001).
[4] H. Narita, J. Glaciol. **26**, 275 (1980).
[5] Z. Watanabe, J. Glaciol. **26**, 255 (1980).
[6] J.A. Åström, M.J. Alava, and J. Timonen, Phys. Rev. E **62**, 2878 (2000).
[7] Thick slabs are usually formed in convex depressions.
[8] P.M. Duxbury, in *Statistical Model for the Fracture of Disordered Media*, edited by H.J. Herrmann and S. Roux (North-Holland, Amsterdam, 1990), Chap. 6.
[9] P.C. Hemmer and A. Hansen, J. Appl. Mech. **59**, 909 (1992).
[10] D. Sornette, J. Phys. I **2**, 2089 (1992).
[11] S.L. Phoenix and I.J. Beyerlein, Phys. Rev. E **62**, 1622 (2000).
[12] W. St. Lawrence, J. Glaciol. **26**, 209 (1980).
[13] R.A. Sommerfeld and H. Gubler, Ann. Glaciol. **4**, 271 (1983).
[14] *Statistical Models for the Fracture of Disordered Media*, edited by H.J. Herrmann and S. Roux (North-Holland, Amsterdam, 1990).
[15] Nature debates URL:http://www.nature.com/nature/debates/earthquake/.